# The Construction of an Energy-dispersive X-Ray Diffractometer for Liquids and Its Application to $CCl_4$

Yoshitada MURATA* and Keiko NISHIKAWA

*Department of Chemistry, Faculty of Science, Gakushuin University, Mejiro, Toshima-ku, Tokyo 171*

(Received July 15, 1977)

An energy-dispersive X-ray diffractometer using a solid-state detector is constructed for the determination of the liquid structure. It has two merits over the usual angle-dispersive diffractometer, *i.e.*, a higher resolution of the $s$-value and a wider measurable $s$-region. The procedure of the data analysis and the results for liquid $CCl_4$ are described. The absorption correction is important in the reflection method. By taking advantage of the energy-dispersive method, it is shown that liquid $CCl_4$ has a long-range correlation at room temperature.

The intensity measurement of X-rays by using a solid-state detector (SSD), since it was introduced by Giessen and Gordon,[1] has been used in various experiments on X-ray scattering, for example, the Compton profile,[2] diffractometry for a single crystal[3] or for a powdered sample,[4] and the determination of the anomalous scattering factor at energies near the absorption edge.[5] However, the X-ray diffraction of liquids has scarcely been studied by means of the energy-dispersive method with the SSD.[6]

The energy-dispersive method in X-ray diffraction is carried out by using white X-rays as the primary beam and the SSD for the energy analysis of the scattered X-rays. In other words, a parameter in the diffraction of a liquid, $s=4\pi \sin\theta/\lambda$ ($\lambda$: wavelength, $2\theta$: scattering angle), *i.e.* the scattering vector, is determined mainly by measuring $\lambda$, while only $\theta$ is changed in the traditional angle-dispersive method.

Energy-dispersive diffractometry has the following merits in comparison with the angle-dispersive one:

(1) A higher resolution of the $s$-value can be obtained. The resolution of the $s$-value is determined by two factors, as is shown by the following relation;

$$\Delta s/s = \Delta E/E + \cot\theta \cdot \Delta\theta. \quad (1)$$

The first term on the right side of Eq. 1 indicates the energy resolution, which is determined by that of the SSD and which varies with the energy.[7] The second term, the angular resolution, is determined by the beam divergence in a collimator system. A small beam divergence is achieved without increasing the time of measurement, since the integrated intensity of the white X-ray radiations is much stronger than that of a characteristic X-ray radiation. Though the diffraction pattern of a liquid forms diffuse halos, a high resolution of the $s$-value is essential if we are to investigate the presence of a long-range correlation.

(2) The fluctuation in the primary beam intensity does not influence the scattering intensity, since scattered photons corresponding to the various $s$-values are collected simultaneously. This is effective in getting relative-intensity curves with high precision.

(3) It is possible to expand the observable region of the $s$-values. This diminishes the termination error in the Fourier transformation, since the diffraction intensities can be measured from small to large $s$-values.

(4) The design of the diffractometer is simple, because no scanning mechanism is necessary. Accessories such as sample holders for high and low temperatures can be mounted easily.

A vertical goniometer is adopted in the present experiment instead of the usual horizontal one, though this selection is not necessarily related to energy-dispersive diffractometry. In the horizontal goniometer, the free surface of a liquid is measured and an X-ray tube and a detector are moved simultaneously on the vertical plane. On the other hand, in the vertical goniometer an X-ray tube or a detector travels on the horizontal plane around the sample; hence, the mechanism of the apparatus is simplified. In addition, the vertical goniometer system makes it possible to measure both reflection and transmission intensities. This expands the measurable region of $s$, especially to very small $s$-values.

However, there are some demerits and difficulties in the energy-dispersive method:

(1) When a liquid specimen includes such elements as heavy metal ions, the fluorescent X-ray emissions disturb the intensity curve.

(2) The absorption and Compton corrections may introduce a significant error.

(3) The intensity curves obtained at different scattering angles must be connected adequately.

The difficulties arising from (2) and (3) were resolved as will be described below.

The present paper will describe the construction of an energy-dispersive diffractometer for liquids. The procedure of the data analysis applied to liquid $CCl_4$ at room temperature will also be described.

## Construction of the Apparatus

The experimental arrangement is shown in Fig. 1.

*Goniometer.* An X-ray tube can be rotated around the vertical axis of a goniometer, which has a $\theta$-$2\theta$ scanning system. An SSD with a heavy cryostat is fixed. The movable range of the tube is from $-20$ to $100°$ in $2\theta$. When the white X-ray radiations from a tungsten tube are used at the target voltage of 45 kV, the scattering intensity is obtained over the range from $s=0.15$ to 30 $Å^{-1}$.

*X-Ray Source.* A fine-focus Phillips tube with a tungsten target is used, because strong white X-rays can be obtained without any disturbance by characteristic X-rays. Although radiations from the tungsten

* Present address: The Institute for Solid State Physics, The University of Tokyo, Roppongi, Minato-ku, Tokyo 106.

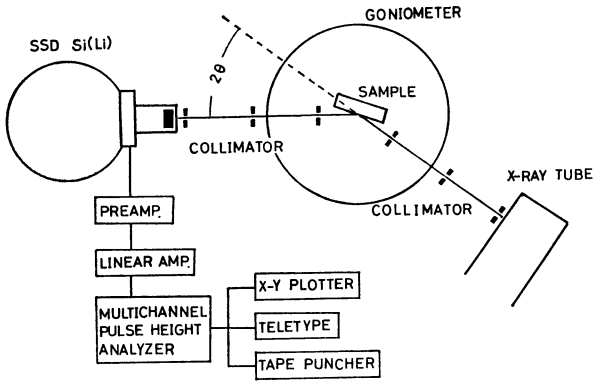


Fig. 1. Shematic diagram of the experimental apparatus. The arrangement for the reflection method is shown.

tube have the $L$ radiations in the 8—11 keV region ($\lambda$=1.2—1.4 Å), as shown in Fig. 5, they do not disturb the present measurements. A high-voltage power supply for X-rays of the Rigaku Denki Co. was used. The stability of the high voltage is better than 0.1%. The X-ray tube was usually operated at 45 kV and 20 mA. However, in the energy-dispersive method it is necessary to measure the spectrum of the incident beam by means of the voltage and collimating system used for the measurement of the intensity scattered from the sample. Since the 20 mA beam is too strong for the direct-beam measurement, we modified the power supply system so as to operate it in the microampere region.

*Detecting System.* The scattered X-rays were analyzed by means of a Si(Li) detector made by the JEOL Co., Tokyo. The energy resolution of the detector $\Delta E$ is 200 eV FWHM at 21.99 keV (Ag $K\alpha_2$), and $\Delta E/E$ is less than 1% in the energy region used in this apparatus ($E$=12—32 keV). It is connected to a linear amplifier (NAIG D-130) and a multichannel pulse-height analyzer (MCA) with 1024 channels (Canberra Model 8100). The gain of the linear amplifier was set so that the energy width per channel of the MCA was about 40 eV.

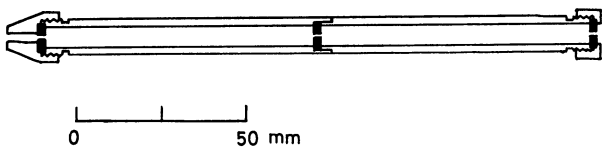


Fig. 2. Collimator. It is 180 mm long and has three apertures with diameter of 1 or 2 mm. Apertures are made of W or Pb.

*Collimator.* The resolution in the $s$-value is determined by two factors, as shown by Eq. 1. The second term of Eq. 1, in which $\Delta\theta$ is the beam divergence, is determined by the design of the collimator system. In this respect it is desirable to use a collimator of an appreciable length and a small diameter. However, this induces a decrease in the X-ray intensities. An optimum condition was realized by keeping the first term in Eq. 1 a little smaller than the second term. We made a couple of collimators 180 mm in length and 1 or

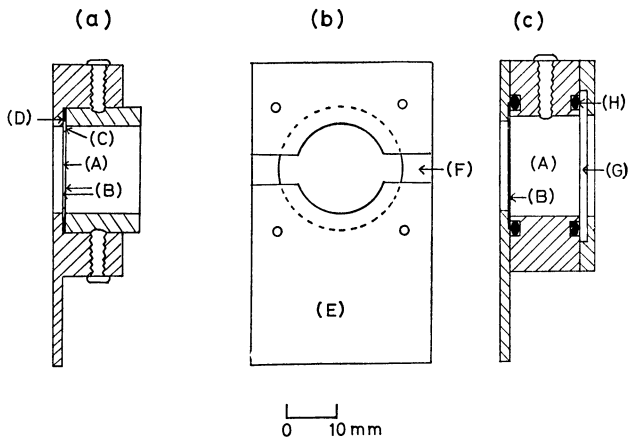


Fig. 3. Sample holder (a) for the transmission method and (b), (c) for the reflection method. (A) sample, (B) Myler film or Be plate, (C) stainless steel ring to determine the thickness of sample (0.5 mm in thickness), (D) rubber ring to seal, (E) stainless steel plate to set the holder to the goniometer, (F) ditch to expand the observable region of the scattering angle, (G) glass plate, (H) O-ring.

2 mm in diameter, as is shown in Fig. 2. Three stages of collimating apertures were effective in getting a well-collimated X-ray beam. If two stages of collimating apertures are used for the measurement; not only is the beam divergence increased, but also a significant error is introduced into the absorption correction in the reflection method, as will be described later. In this system, $\Delta\theta$ is 0.3 or 0.6°. The latter value, 0.6°, is used only at large scattering angles, which correspond to small cot $\theta$ values.

*Sample Holder.* The sample holders are shown in Fig. 3. Figure 3(a) illustrates a sample holder for the transmission method, which is used for the measurements at small scattering angles. Myler films (20 $\mu$m thick) or Be thin plates (0.2 mm thick) were used for the window of the sample holder. The window was sealed with epoxide resin, which is not insoluble in the $CCl_4$ sample. For other organic liquid samples, the window was made by welding the Be plate with a Cu block by diffusion bonding in a vacuum oven. A sample holder for the reflection method is shown in Figs. 3(b) and (c).

## Measurements of $CCl_4$

Carbon tetrachloride is one of the simplest molecules which are liquid at room temperature, and so it has been studied well.[8-11] Therefore, it was selected as a suitable sample for the first experiment with this apparatus. The carbon tetrachloride molecule has a nearly spherical electron cloud and has no heavy atoms to disturb the energy distribution curve by fluorescent X-rays in the energy-dispersive measurements.

In order to obtain the relation of the energy *vs.* the channel number in the MCA, the fluorescent X-rays from Ba, Ag, Mo, and Cu were measured. The results are shown in Fig. 4. The channel numbers of these peaks in the MCA were fitted to the energies of the

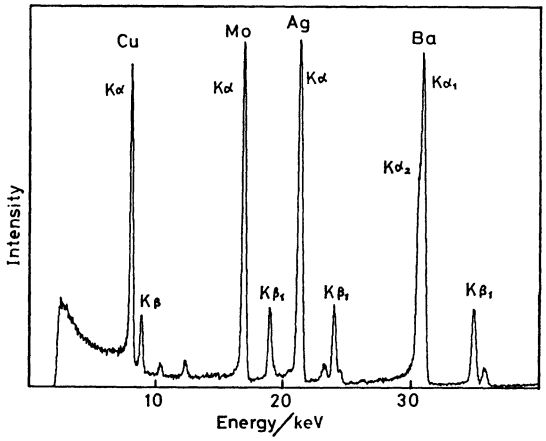


Fig. 4. A spectrum of the fluorescent X-rays from several targets for the calibration of the energy scale in the MCA.

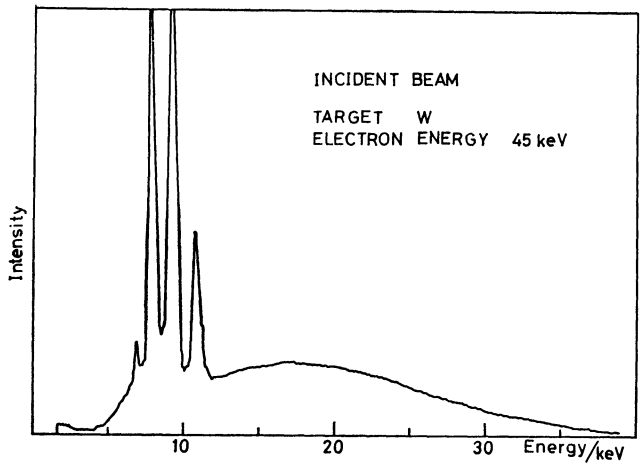


Fig. 5. A tungsten spectrum for the incident white X-rays. The X-ray source was operated at 45 kV and 10 μA.

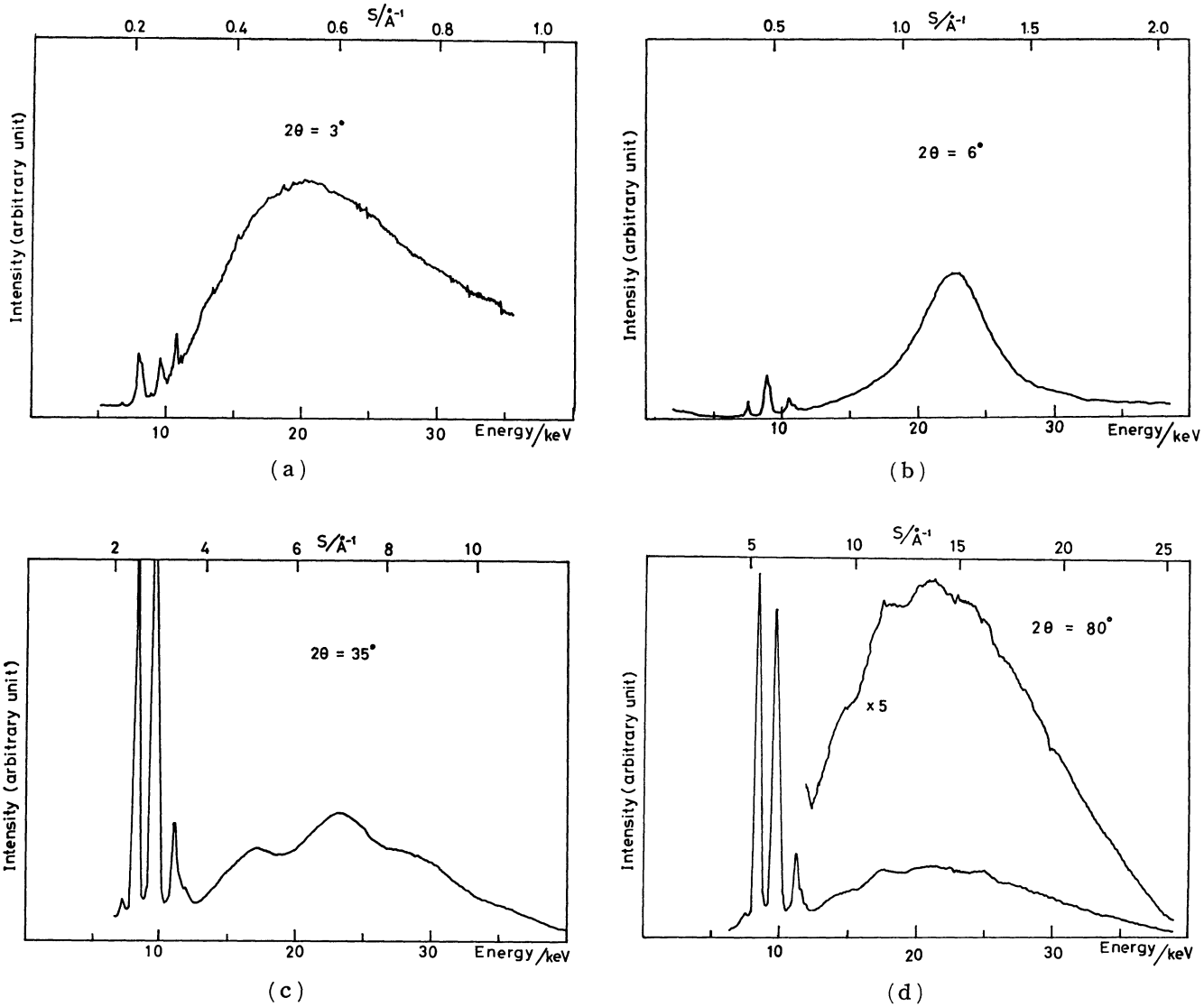


Fig. 6. Scattered intensities from liquid $CCl_4$ at room temperature. (a) $2\theta=3°$, (b) $2\theta=6°$, (c) $2\theta=35°$, (d) $2\theta=80°$; (a), (b) transmission method, (c), (d) reflection method.

corresponding characteristic X-ray radiations by using a table by Bearden.[12] Since the doublets of Cu $K\alpha$, Mo $K\alpha$, and Ag $K\alpha$ can not be separated by the SSD, the weighted mean energy of $K\alpha_1$ and $K\alpha_2$ was used. The radiations of $K\alpha_1$, $K\beta_1$ in Ba and $K\beta_1$ in Mo and Ag were also used for the calibration. A linear relation between the energy and the channel number was obtained.

The observed energy distribution curve of the incident beam is shown in Fig. 5. This spectrum was obtained from the tungsten target operated at 45 kV and 10 $\mu$A.

X-Rays scattered from liquid $CCl_4$ were collected at the scattering angles of $2\theta=1.5$, 3, 6, 18, 35, 56, and 80°. The specimen was held at room temperature. The data for $2\theta=1.5$, 3, 6, and 18° were measured by means of the transmission method. The reflection method was applied to $2\theta=35$, 56, and 80°. The setting of $2\theta=1.5$, 3, 6, 18, 35, 56, and 80° made it possible to measure $s=0.15$—0.41, 0.30—0.83, 0.56—1.86, 1.75—4.91, 3.78—9.45, 5.90—14.8, and 8.08—23.0 Å$^{-1}$ respectively. The measuring time at each scattering angle was $5\times10^4$—$10^5$ s, and more than 4000 counts per channel were obtained. The diffraction patterns collected in the MCA are shown in Fig. 6. The $s=0.30$—0.82 Å$^{-1}$ region, $2\theta=3°$, is shown in Fig. 6(a), where no halo due to interference between atoms appears. In Fig. 6(b), $2\theta=6°$, the peak at $s=1.2$ Å$^{-1}$ indicates the first halo due to interference. Figures 6(c) and (d) show the diffraction patterns obtained at $2\theta=$ 35 and 80° respectively; we can see several halos whose amplitudes gradually decrease as the $s$-value increases.

The scattering from the Myler film or the Be thin plate of the window of the sample holder was also measured. This curve was denoted as $I_w$. The magnitude of $I_w$ was about 5% of the total scattering intensity from liquid $CCl_4$.

## Data Analysis

*Smoothing and Normalization.* Smoothing was done by adding the counts collected in each group of five channels, because the resolution of the SSD is about 200 eV and the linear amplifier was so set that the energy width for each channel in the MCA was about 40 eV. The counts at each point after smoothing were more than $2\times10^4$, which were sufficient to diminish the statistical random error. Each scattering intensity from which the intensity, $I_w$, was subtracted was divided by the energy distribution curve of the incident beam (normalization).

*Absorption Correction.* The most important correction in energy-dispersive diffractometry of liquids is the absorption correction, because the linear absorption coefficient, $\mu$, changes with the energy of the X-rays and the effect of the path length in scattering must also be taken into account.

We checked whether or not the calculated values of $\mu$ agreed with the observed ones. The value of $\mu$ was calculated as follows

$$\mu/\rho = \tau + \sigma, \tag{2}$$

where $\rho$ is the density of the liquid, $\tau$ is the photo-electric absorption and $\sigma$ is the absorption due to the Compton effect. The empirical relation of $\tau$ is given by

$$\tau = C\lambda^3 - D\lambda^4, \tag{3}$$

where $\lambda$ is the X-ray wavelength in Å and where $C$ and $D$ are constants characteristic of atoms. These constants are tabulated in the International Tables. The $C$'s for carbon and chlorine are 1.22 and 33.4 respectively, and the $D$'s are 0.0142 and 3.03 respectively.[13] The absorption due to the Compton effect was given by Klein and Nishina[14] as

$$\sigma = \frac{2\pi e^4}{m^2c^4}\left[\frac{1+\alpha}{\alpha^2}\left\{\frac{2(1+\alpha)}{1+2\alpha}-\frac{1}{\alpha}\ln(1+2\alpha)\right\}+\frac{1}{2\alpha}\ln(1+2\alpha)-\frac{1+3\alpha}{(1+2\alpha)^2}\right], \tag{4}$$

where $\alpha=h/mc\lambda$ and $m$ is the electron rest mass.

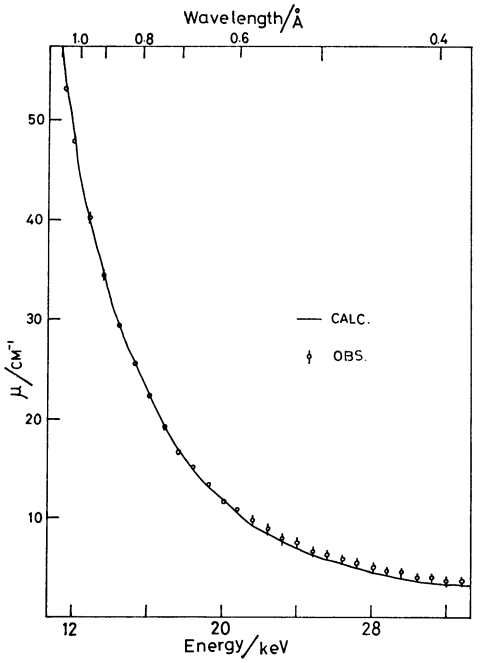


Fig. 7. Calculated and observed linear absorption coefficient, $\mu$, of liquid $CCl_4$.

The observed values of $\mu$ were measured from the trasmittance of the sample at $\theta=0°$. The observed and calculated values are shown in Fig. 7. A good agreement was obtained except in the high-energy region, where the latter values are somewhat smaller than the former. The observed values were used for the data analysis.

The path length in the case of the transmission method can be estimated easily as shown in Fig. 8(a), because the $\theta$-$2\theta$ scanning system has been used in this experiment. The path length is given by $t\cdot\sec\theta$, where $t$ is the thickness of the sample. The absorbed intensity, $I'$, is given by

$$I' = I\exp(-\mu t\sec\theta), \tag{5}$$

where $I$ is the intensity without absorption.

In the reflection method, the absorption correction is complicated, because the path length differs depending on the position at which the X-ray is scattered, as shown in Fig. 8(b). The absorbed intensity in the

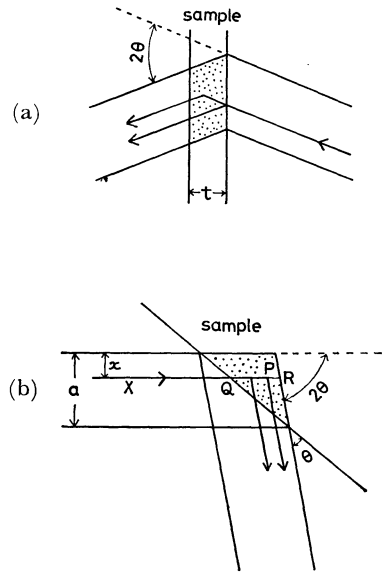


Fig. 8. Path length for the absorption correction. (a) Transmission method. The path length is always $t$ sec $\theta$ wherever X-rays are scattered. (b) Reflection method. The path length depends on the position where X-rays are scattered. The X-rays scattered in the dotted area reach the detector.

reflection method is given by

$$I' = I\frac{a^2}{4\mu}\left[\frac{\pi}{2}-\int_{\pi/2}^{3\pi/2}\cos^2\phi\,\exp\{-\mu a(1+\sin\phi)/\sin 2\theta\}\mathrm{d}\phi\right], \quad (6)^{**}$$

where $a$ is the beam diameter on the sample. The derivation of this equation is given in the Appendix.

For the absorption correction, it is important to estimate the effective value of the beam diameter on the sample. A criterion for the estimation of the effective beam diameter is that the background intensity for the observed intensity curve after the Compton correction is proportional to the calculated curve of $\sum_n f_n(s)^2$, where $f_n(s)$ is the atomic scattering factor for a component atom, $n$, of the molecule. The background intensity means a monotonically decreasing curve corresponding to $\sum_n f_n(s)^2$. The effective beam diameter was 1.2 times as large as the diameter of the aperture at $2\theta=35°$ and grew a little larger as the scattering angle increased. The presence of multiple scattering is probably the reason for the dependence of the effective diameter on the scattering angles. In this apparatus, each collimator has three stages of apertures, as shown in Fig. 2. When each collimator has only two apertures, the effective value of the beam diameter can not be obtained. Figure 9 indicates the importance of the estimation of the effective value of the beam diameter by showing three curves of $I'/a^2I$ in Fig. 6. Curve (a) in Fig. 9 shows the contribution from the first term in the brackets. This is the usual absorption correction in the reflection method for a strong absorption case, in which

** The reflection from the wall of the sample holder is ignored in Eq. 6. This is justified in the present experiment.

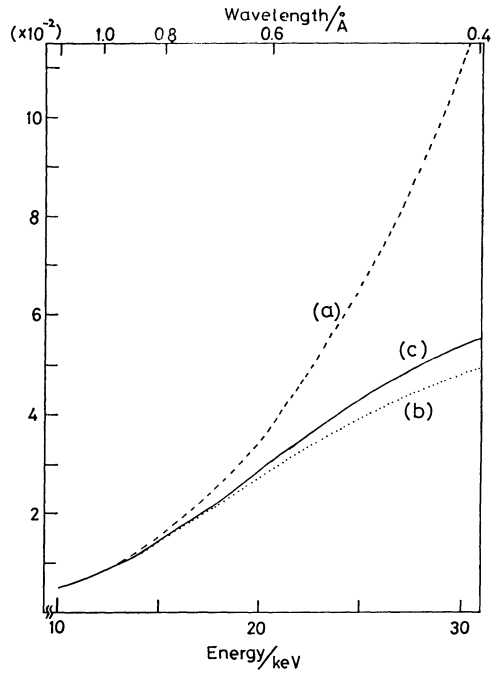


Fig. 9. Curve (a) (broken line) denotes $\pi/8\mu$. Curves (b) (dotted line) and (c) (full line) are

$$\frac{1}{4\mu}\left[\frac{\pi}{2}-\int_{\pi/2}^{3\pi/2}\cos^2\phi\cdot\exp\{-\mu a(1+\sin\phi)/\sin 2\theta\}\mathrm{d}\phi\right]$$

where $a$ is 1.0 mm in (b) and 1.2 mm in (c).

$a$ is much larger than $\mu^{-1}$. Curve (b) shows the result for $a=1$ mm, in which $a$ agrees with the diameter of the apertures. Curve (c) is calculated using the effective beam diameter on the sample in which $a=1.2$ mm. We can recognize from Fig. 9 that the second term in the brackets of Eq. 6 is important for the absorption correction. The second term becomes more significant as the X-ray energy increases (*i.e.* $\mu$ decreases) and as $a$ decreases. Therefore, this correction is characteristic of this energy-dispersive method. The curvature of these curves influences the background intensity of the observed intensity curve.

*Compton Correction and Absorption Intensity.* The scattered intensity, $I(s)$, after the absorption correction is given by

$$I(s) = K[\sum_n f_n(s)^2 + i_1(s) + i_2(s) + kI_C I_0(\lambda)/I_0(\lambda')], \quad (7)$$

where $I_C$ is the intensity of the Compton scattering, $k$ is the recoil factor, and $K$ is the conversion factor from the experimental to absolute intensity (in electron units). $I_0(\lambda)$ and $I_0(\lambda')$ are the intensities of the incident beam at the wavelengths of $\lambda$ and $\lambda'$ respectively, and $\lambda'-\lambda$, the Compton shift, is given by $(h/mc)(1-\cos 2\theta)$. The first term in Eq. 7 represents the scattering from individual atoms. The second term is called the molecular term, which is the interference from each atom pair within a molecule. The third term represents the interference from atom pairs between different molecules.

The molecular term for $CCl_4$ is represented by

$$i_1(s) = 8f_C f_{Cl}\frac{\sin sr_{C-Cl}}{sr_{C-Cl}}\exp\left(-\frac{l^2_{C-Cl}}{2}s^2\right) + 12f^2_{Cl}\frac{\sin sr_{Cl-Cl}}{sr_{Cl-Cl}}\exp\left(-\frac{l^2_{Cl-Cl}}{2}s^2\right), \quad (8)$$

where $l_{ij}$ denotes the root mean-square amplitude due to the vibration of the atom pair around the mean internuclear distance, $r_{ij}$. Since $i_2(s)$ vanishes at large $s$-values, the absolute intensities are obtained by adjusting the experimental intensities to the calculated intensities, which are obtained by adding the first, second, and fourth terms of Eq. 7 at large $s$-values. In the calculation, the $r_{C-Cl}$, $r_{Cl-Cl}$, $l_{C-Cl}$, and $l_{Cl-Cl}$ values obtained by gas electron diffraction of $CCl_4$[15] were used and the intensities of the Compton scattering calculated by Cromer[16] were employed.

The conversion factor from the experimental to absolute intensity, $K$, were easily obtained for $2\theta=35$, 56, and 80°; the agreement of the intensity curves in the overlapping region was good. In the cases of $2\theta=$ 1.5, 3, 6, and 18°, an approximation of $i_2(s)=0$ is not so good. Accordingly, each intensity curve was successively connected with that of $2\theta=35°$ after the absorption correction. Then, $K$ was obtained for each intensity curve.

The total coherent intensity

$$I_{co}(s) = \sum_n f_n(s)^2 + i_1(s) + i_2(s), \quad (9)$$

was obtained by subtracting the fourth term in $I(s)/K$ of Eq. 7. The Compton correction was carried out by using the calculated values reported by Cromer.[16] Figure 10 shows the observed coherent intensity of liquid $CCl_4$ at room temperature, together with the calculated value corresponding to independent atoms of carbon tetrachloride, $\sum_n f_n(s)^2$.

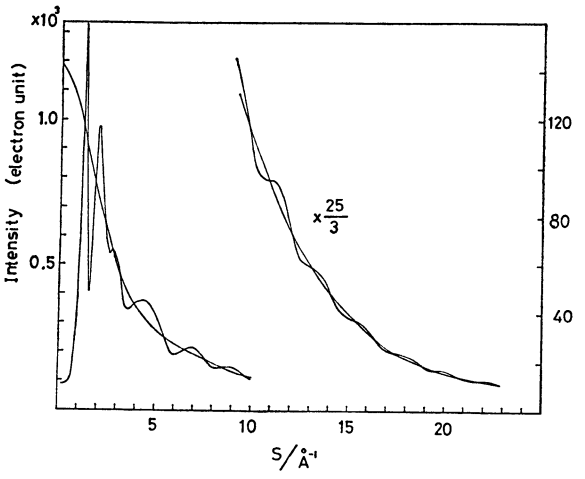


Fig. 10. Observed total coherent intensity $I_{co}$ for liquid $CCl_4$ at room temperature and calculated one assuming that atoms in $CCl_4$ are independent.

The weighted structure function, $si(s)$, of liquid $CCl_4$ is shown in Fig. 11, where $i(s)=i_1(s)+i_2(s)$ is the reduced intensity. An electronic pair correlation function, $g_e(r)$, was defined by the Fourier transformation of $si(s)$;

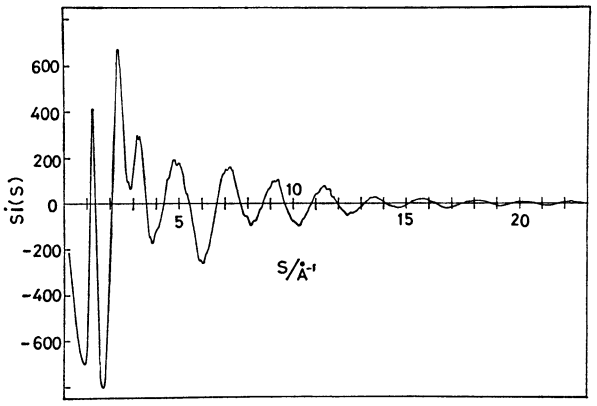


Fig. 11. Weighted structure function $si(s)$ for liquid $CCl_4$ at room temperature.

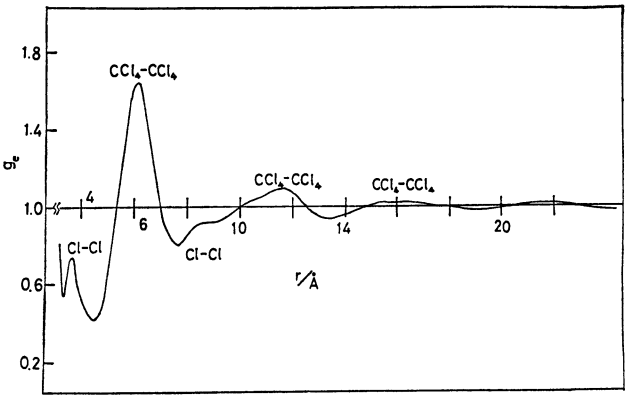


Fig. 12. Electronic pair correlation function $g_e(r)$ for liquid $CCl_4$ at room temperature.

$$g_e(r) = \frac{1}{2\pi^2 r\rho_0\sum_n Z_n^2}\sum_{s=0}^{s_{max}} si(s)\sin sr\cdot\Delta s + 1, \quad (10)$$

where $\rho_0$ is the bulk liquid density and $Z_n$ is the atomic number of a component atom $n$ (Fig. 12). In the transformation, only the observed values of $si(s)$ were used throughout the whole region except for $s=0.05$ and 0.10, at which $si(s)$ were extrapolated. This extrapolation can not cause any significant error, since $I_{co}$'s have a constant value at these positions, as shown in Fig. 10. The $\Delta s=0.05$ Å$^{-1}$ interval and $s_{max}=23.0$ Å$^{-1}$ were used. This range of $s$ is sufficient to eliminate the termination error for Fourier transformation.

The electronic pair correlation function calculated from Eq. 10 is different from the usual pair correlation function, which corresponds to the distribution of the nucleus. The former expresses the distribution of the electron, since, in the present paper, $i(s)$ is $\sum_{i\neq j} f_i f_j(\sin sr/sr)\exp(-l_{ij}^2 s^2/2)$. Therefore, the mean square amplitude obtained directly from Fig. 12 includes the effect of the distribution of the electron cloud. If we try to obtain the usual pair correlation function, $g(r)$, by multiplying $(\sum_n f_n(s)^2)^{-1}$, which is a convenient factor to change from the electron density to the nuclear density, some errors may be introduced by the correction.

## Results and Discussion

Figure 12 shows that liquid $CCl_4$ at room temperature

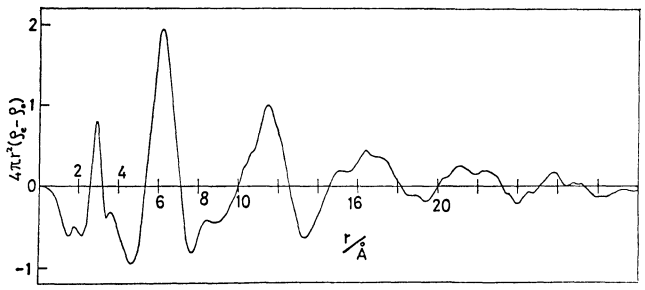


Fig. 13. Electronic radial distribution function from which the bulk density was subtracted, $4\pi r^2(\rho_e-\rho_0)$.

has a long-range correlation. In order to see it more clearly, the electron radial distribution function from which the bulk density was subtracted, $4\pi r^2(\rho_e-\rho_0)$, is shown in Fig. 13. The peak at 6.3 Å corresponds to the first nearest neighbor molecules, while the three other peaks, appearing at 11.4, 16.3, and 21.5 Å, are due to interference between molecules. The interference with the fourth nearest neighbor molecules has a distinct peak in the radial distribution function.

Though information on the long-range order in the liquid is confined mainly to the $s\lesssim 2$ region of the weighted structure function, it is clearly recognized elsewhere. Figure 11 shows that the intensity curve has a fine structure with a short periodicity at small $s$-values.*** The fine structure near the top and bottom of the halos, such as those at $s=3.2$ and 4.7 Å$^{-1}$, was reproducible not only in repeated measurements but also in measurements at different scattering angles. The periodicity in this fine structure was 0.2—0.3 Å$^{-1}$, which was larger than the estimated resolution in the $s$-value ($\Delta s=0.14$ Å$^{-1}$ at these $s$-values) in the present experiment. The difference between the collected counts of the top and the bottom of these small waves was about 500 counts, more than the statistical radom error ($\sqrt{n}=170$; $n=3\times10^4$). In the energy-dispersive method, the scattered intensity is scarcely influenced by the fluctuation in the incident-beam intensity. Therefore, the statistical random error given by the square root of the total counts at each position is the main origin of the noise. Though attention has not yet been paid to this fine structure in the liquid structure analysis, the fine structure may indicate that $CCl_4$ in the liquid phase at room temperature has a long-range order.

The scattering intensities at small $s$-values contain information about the density fluctuation. The decrease in the total coherent intensity near $s=0$ shown in Fig. 10 is due to the intermolecular correlation. The fluctuation in the number density of a liquid can be estimated from the absolute value of the total coherent intensity at $s=0$, which is obtained by extrapolating the observed intensities. A constant value in the intensity, $I_{co}$, was obtained at small $s$-values, as shown in Fig. 10, so that the extrapolation to $s=0$ is easy. According to liquid theory,[17,18] the mean square of the fluctuation in the number density is given by

$$\langle(N_v-\langle N_v\rangle)^2\rangle = \langle N_v\rangle I_{co}(0)/(\sum_n Z_n)^2, \qquad (11)\dagger$$

where $N_v$ is the number of molecules in a small volume $v$, $\langle N_v\rangle$ means the average value of $N_v$, $I_{co}(0)$ is the total coherent intensity at $s=0$ in electron units (e.u.), and $Z_n$ is the atomic number. As shown in Fig. 10, $I_{co}(0)$ equals 87 e.u. Hence, $\langle(N_v-\langle N_v\rangle)^2\rangle$ was $9.9_5\times10^{-5}v$ in Å units. This means that $\langle(N_v-\langle N_v\rangle)^2\rangle$ becomes unity when $v$ is $1.00\times10^4$ Å$^3$, in which there are 63 molecules, on the average. In other words, there are $63\pm1$ molecules in $1.00\times10^4$ Å$^3$ and $252\pm2$ molecules in $4.00\times10^4$ Å$^3$. Of cource, this estimation includes some error because the absolute intensity at small $s$-values was not measured directly, but obtained successively from that observed at $2\theta=35°$. This value is, though, in good agreement with the compressibility of liquid $CCl_4$ $\kappa=10.34\times10^{-11}$ cm$^2$ dyn$^{-1}$ (at 20 °C).[19] The details of the results for liquid $CCl_4$ including the temperature dependence will be reported elsewhere.[20]

Finally, let us compare this apparatus with a usual angle-dispersive diffractometer.[21] The resolution in the $s$-value is given by Eq. 1. The first term of Eq. 1, $\Delta E/E$ ($\approx0.01$), in this apparatus is much larger than that in the usual one. On the other hand, the $\Delta s/s$ in the usual apparatus is at least twice as large as that in the present one, because $\cot\theta\cdot\Delta\theta\lesssim0.01$ over the range from $s=1.5$ to 30 Å$^{-1}$ in this apparatus, since the collimating system is so designed that the beam divergence, $\Delta\theta$, is 0.3 or 0.6°, in contrast to the usual 2—4°. This difference in $\Delta s/s$ is significant, because the periodicities of the fine structures observed in the scattering intensity value, $si(s)$, $\Delta s=0.2$—0.3 Å$^{-1}$, are about twice as large as the resolution of this apparatus. Moreover, these fine structures are hardly influenced at all by the intensity fluctuation of the primary beam in the present experimental method.

Diffraction intensities can be obtained over the range from $s=0.15$ to 30 Å$^{-1}$ in the present apparatus by using white X-rays. On the contrary, the intensities in the usual apparatus are taken $s$-values from 0.4 to 16 Å$^{-1}$, in which the scattering angle, $2\theta$, is varied from 4 to 140° if Mo $K\alpha$ ($\lambda=0.7107$ Å) is used. Therefore, the electronic radial distribution function without the termination error in Fourier transformation can be obtained with the present apparatus by using only the observed intensities.

The total time required for collecting the data with this apparatus is comparable to that with the usual one. Nevertheless, a higher resolution in $s$-value and a wider region of observable intensity can be obtained with this apparatus.

The authors wish to express their thanks to Dr. Teruo Nomura, Rikkyo University, for his collaboration, and

*** The fine structure at large $s$-values is random noise, because the ratio of the reduced intensity $i(s)$ to the total scattering intensity is small.

† In the above discussions, we have done the calculations considering the atomic distribution, but in the estimation of the density fluctuation we must consider the molecular distribution by taking $(\sum_n Z_n)^2$ instead of $(\sum_n Z_n^2)$ as the denominator.

to Dr. Tomoe Fukamachi and Prof. Sukeaki Hosoya, The Institute for Solid State Physics, for their discussion and for allowing us to do our preliminary experiments in their laboratory. We also would like to thank Prof. Kozo Kuchitsu, The University of Tokyo, for permission to use a computer program for gas electron diffraction and Messrs. Kyozuka, Kimura, Kato, and Yamada, JEOL Co., for making the detector. Thanks are also due to Dr. Masahiro Kotani of Gakushuin University for reading the manuscript. The present work was partially supported by Grants-in-Aid for Scientific Research and a Grant-in-Aid for Developmental Scientific Research from the Ministry of Education.

## Appendix

The derivation of Eq. 6 is as follows. In Fig. 8(b), when the beam, X, is scattered at the point P, the contribution of absorption becomes $\exp(-2\mu\overline{PQ})$, where $\overline{PQ}$ means the distance between P and Q. Because P can change from the point Q to R in the case of the X beam, the possible range of $\overline{PQ}$ becomes from 0 to $(a-x)/\sin 2\theta$, where $x$ is as is shown in Fig. 8(b) and varies from 0 to $a$. The total contribution of absorption in the X beam is given by

$$A_x = \int_0^{(a-x)/\sin 2\theta} \exp(-2\mu y)\mathrm{d}y$$
$$= \{1-\exp(-2\mu(a-x)/\sin 2\theta)\}/2\mu.$$

The absorption correction for incident and scattered parallel beams, the diameters of which are equal to $a$, is given by

$$A_{\text{total}} = \int_0^a 2\sqrt{\left(\frac{a}{2}\right)^2-\left(\frac{a}{2}-x\right)^2}A_x\mathrm{d}x.$$

If we put $1-2x/a=\sin\phi$, we get

$$A_{\text{total}} = \frac{a^2}{4\mu}\int_{\pi/2}^{3\pi/2}\cos^2\phi\,[1-\exp\{-\mu a(1+\sin\phi)/\sin 2\theta\}]\mathrm{d}\phi$$
$$= \frac{a^2}{4\mu}\left[\frac{\pi}{2}-\int_{\pi/2}^{3\pi/2}\cos^2\phi\exp\{-\mu a(1+\sin\phi)/\sin 2\theta\}\mathrm{d}\phi\right].$$

## References

1) B. C. Giessen and G. E. Gordon, *Science*, **159**, 973 (1968).
2) T. Fukamachi, S. Hosoya, Y. Hosokawa, and H. Hirota, *Phys. Status Solidi A*, **10**, 437 (1972).
3) B. Buras and J. Stan Olsen, *Acta Crystallogr., Sect. A*, **31**, 327 (1975).
4) B. Buras, J. Chawaszczewska, S. Szarras, and Z. Szmid, (1968), Report 894/II/PS, Institute of Nuclear Research, Warsaw; R. Uno and J. Ishigaki, *J. Appl. Crystallogr.*, **8**, 578 (1975).
5) T. Fukamachi and S. Hosoya, *Acta Crystallogr., Sect. A*, **31**, 215 (1975).
6) J. M. Prober and J. M. Schultz, *J. Appl. Cryst.*, **8**, 405 (1975).
7) T. Fukamachi, S. Hosoya, and O. Terasaki, *J. Appl. Crystallogr.*, **6**, 117 (1973).
8) A. Eisenstein, *Phy. Rev.*, **63**, 304 (1943).
9) R. W. Gruebel and G. T. Clayton, *J. Chem. Phys.*, **46**, 639 (1967).
10) A. H. Narten, M. D. Danford, and H. A. Levy, *J. Chem. Phys.*, **46**, 4875 (1967).
11) A. H. Narten, *J. Chem. Phys.*, **65**, 573 (1976).
12) J. A. Bearden, *Rev. Mod. Phys.*, **39**, 78 (1967).
13) "International Tables for X-Ray Crystallography," Kynoch Press, Vol. III, Birmingham (1962), p. 171.
14) O. Klein and Y. Nishina, *Z. Phys.*, **52**, 853 (1929).
15) Y. Morino, Y. Nakamura, and T. Iijima, *J. Chem. Phys.*, **32**, 643 (1960).
16) D. T. Cromer, *J. Chem. Phys.*, **50**, 4857 (1969).
17) M. Toda, "Ekitairon," Iwanami, Tokyo (1955), p. 38.
18) Y. Murata, *J. Cryst. Soc. Jpn.*, **17**, 36 (1975).
19) R. E. Gibson and O. H. Leoffer, *J. Am. Chem. Soc.*, **63**, 898 (1941).
20) K. Nishikawa and Y. Murata, *Chem. Phys. Lett.*, (to be published).
21) H. A. Levy, M. D. Danford, and A. H. Narten, ORNL Rept. ORNL-3960 (1962).